Phase Behavior and Percolation Studies on Microemulsion System Water/SDS + Myrj45/Cyclohexane in the Presence of Various Alcohols as Cosurfactants

Arti Dogra and A. K. Rakshit*

Department of Chemistry, Faculty of Science, The Maharaja Sayajirao University of Baroda, Baroda 390 002, India

Received: January 7, 2004; In Final Form: April 20, 2004

The phase behavior of a water/mixed surfactant/*n*-propanol/cyclohexane system was studied at various temperatures of 30, 40, and 50 °C. The mixed surfactant−*n*-propanol ratio was kept arbitrarily constant at 0.5. The mixed surfactant was a mixture of anionic sodium dodecyl sulfate and nonionic polyoxyethylene monostearate (Myrj45) at various mole ratios. The effect of salt on the phase behavior was also studied at those temperatures. Phase volume and optimal salinity were obtained for different molefractions of SDS in mixed systems. The water-induced percolation of water/SDS + Myrj45(1:1)/cyclohexane has been studied in detail in the presence of various alcohols as cosurfactants. The percolation threshold was obtained by using the sigmoidal Boltzman equation. The results have been examined in light of the appropriate scaling equation, and the activation energy for the percolation process was computed.

Introduction

A microemulsion is a low viscosity macroscopically single phase fluid, resulting from the mutual solubility of water and oil. Such mutual solubility requires the addition of one or several surface active agents so that a water in oil (w/o) or an oil in water (o/w) microemulsion may be obtained according to the component's nature and the concentration ratio. Many systems require the presence of alcohol and /or salt for their formation and stability.[1−4] The resulting systems may have four or five components, and therefore, data analysis is often difficult. It is well-known that certain mixtures of surfactants can provide better performance than pure surfactants for a wide variety of applications[5−7] and thus it is expected that enhanced solubilization of water in a w/o microemulsion may be achieved with certain surfactant mixtures. The topology of the oil and water domains can vary, depending on the composition and temperature.[8] In most of their applications, surfactants are used in the presence of additives to improve their properties. Among the large number of additives revealed by a literature survey, alcohols hold a special place, being by far the most frequently used. The oil crisis and the suggested use of microemulsions in tertiary oil recovery to improve the yield of oil fields greatly stimulated the research on every possible aspect of the physical chemistry of surfactant + alcohol systems: partition of alcohols between the micelle pseudophase and intermicellar phase, surface tension of the mixed solutions, degree of ionization, aggregation number, and micelle dynamics in the presence of alcohols, etc. Conductance measurements have been used to assess microemulsion formation and probe the structural changes occurring in such systems. The sharp increase in conductivity (over orders of magnitude) observed in some water-in-oil microemulsions having spherical droplet structure has been characterized as a percolation of identical conducting objects, randomly distributed in an insulating medium.[4−10] A large and steep increase of the conductance in some w/o microemulsions[5,9−11] is observed when the volume fraction of the dispersed phase (water + surfactant) or the temperature is increased. This is known as percolation.[12] The percolation threshold ϕ_w^p corresponds to the formation of the first infinite cluster of droplets. The number of such clusters increases very rapidly above the percolation threshold, giving rise to the observed changes of properties, in particular, to the increase of conductance. It is generally considered that, during percolation water microdroplets come in close contact and charge carriers propagate by hoping between droplets[13−15] and/or transfer of counterions from one droplet to another through water channels.[13] Also, a phase transition from a reversed micellar to a bicontinuous microemulsion topology will also lead to a sharp conductivity increase.[14] Such transition usually occurs in systems formulated with low concentrations of surfactant and comparable volume fractions of water and oil. Microemulsions formed by nonionic oligo(ethylene oxide) surfactants exhibit such behavior.[8,16] Hence in continution of our earlier work[17−23] we have studied the present system. Cyclohexane (oil) is often used as a solvent in the chemical industry and in the laboratory. Hence we thought that a cyclohexane microemulsion may be important and useful in reducing the use of organic solvent. The phase diagrams of ionic−nonionic surfactant microemulsions at 1:3, 3:1, 1:1, and 0:1 ratios have been constructed and the effect of various cosurfactants (alcohols) has been studied on the percolation behavior for the w/o microemulsion formed by mixed surfactant SDS + Myrj-45 (1:1 w/w) system.

Materials and Methods

Materials. Polyoxyethylene monostearate (Myrj45) of Sigma was used without further purification. Sodium dodecyl sulfate (SDS) procured from Qualigens was recrystallized from alcohol till a surface tension vs log concentration curve did not show any minimum. Different alcohols called cosurfactants, viz., *n*-propanol (PrOH), *n*-butanol (BuOH), *n*-pentanol (PenOH), *n*-hexanol (HexOH), 2-propanol (2-PrOH), and 2-butanol (2-BuOH) of AR grade were obtained from Suvidhinath Laboratory, Baroda, India, and 1,3-propandiol (1,3-PrOH) and 1,5-

* Corresponding author. E-mail: rakshitak@indiatimes.com, akrakshi@yahoo.co.in.

10.1021/jp049928u CCC: $27.50
Published on Web 06/11/2004

pentanediol (1,5-PenOH) were obtained from Fluka and were dried with anhydrous calcium sulfate and distilled before use. They were stored in the presence of molecular sieves. NaCl (Analar) was obtained from Qualigens. Cyclohexane was purchased from S. D. Fine Chem. Ltd. It was passed through a chromatographic column of silica gel in the lower section and basic alumina in the upper section to remove aromatic impurities and then subjected to distillation prior to use. Doubly distilled water was used to prepare sample solutions.

Methods. For volume-induced percolation measurements, a mixture of amphiphile and cyclohexane was taken in a beaker with $s = 3.2 =$ [oil]/[surfactant], and water was added in aliquots from a microburete with constant stirring. The amphiphile was a mixture of surfactant and cosurfactant (1:2 w/w). The conductance was measured by Weltronix conductivity bridge, at each addition after allowing sufficient time for the attainment of constant temperature. A dip type cell (cell constant 1.01 cm^{-1}) was used. The conductance was then plotted as a function of volume fraction of water. Measurements were taken at 30, 40, and 50 °C temperatures. Water was added until a large increase in conductance followed by a mild increase in the form of sigmoidal variation was observed. The results helped to obtain the threshold stage of percolation.

The boundaries of the single phase microemulsion region were determined by a titration technique. A known amount of oil or water was taken with the amphiphile in stoppered test tubes and kept in a thermostated water bath of required temperature (±0.1 °C). These mixtures were then titrated with water or oil, respectively, from a microburet. Studies at higher temperatures were done with stoppered test tubes closed with Teflon tape. The measurements were checked for reproducibility and the compositions were expressed in weight percent to construct the phase diagrams on triangular coordinates. The area of the microemulsion phase was quantitatively determined using a planimeter.

Interfacial tension (IFT) was measured by using the spinning drop tensiometer (University of Texas, Austin Model No. 500). The interfacial tension was measured between the two phases in equilibrium with either water or oil. The concentration of amphiphile, water, and oil varied from (27.25, 24.92, 47.83%) to (40.05, 36.61, 23.34%), respectively. The capillary tube was filled with the higher density fluid, and the drop was made with lower density liquid. The tube was then spun at different speeds in such a way that the droplet inside the tube was elongated to approximately 4 times its diameter. The diameter was measured by a traveling microscope mounted on the tube. The IFT of the system was computed by using the following equation:

$$\mathrm{IFT} = \frac{1.234\Delta\rho D^3}{P^2(1.332)^3} \qquad (1)$$

where $\Delta\rho$ is the density difference, D is the minor axis of the elongated droplet, 1.332 is the correction factor for the refractive index of the glass of the capillary tube, and P is the time in milliseconds per revolution; 1.234 is the instrument constant. The density of the fluids were determined by using a pycnometer.

Results and Discussion

Figure 1a−e shows the representative phase diagram of different weight fractions of surfactants (SDS + Myrj45: 1:0, 3:1, 1:1, 1:3, and 0:1 mol/mol)/*n*-propanol/water/cyclohexane system at 40 °C, respectively. In Figure 1e (i.e., the water/Myrj45 + *n*-propanol/cyclohexane system), the upper portion is the monophasic microemulsion (μE) region (1ϕ). The lower portion is the liquid/liquid (L/L) biphasic region (2ϕ) where the microemulsion is in equilibrium with excess oil. In Figure 1b−d the middle portion is the monophasic μE region. In these cases the surfactant was the mixed SDS + Myrj45 at various composition ratios (see legend). Phase diagram patterns are similar at all temperatures studied. Generally, nonionic surfactants are found to be sensitive to temperature,[24,25] as the solubility of the surfactant decreases with an increase of temperature. Hence various phase changes with change in temperature was expected in this case. However, in this particular system, the phase diagram remained reasonably unchanged with temperature both for the pure Myrj45 system (Figure 1e) and also the mixed SDS + Myrj45 system (Figure 1b−d). For the pure Myrj45 system (Figure 1e) it remains simple with only monophasic and biphasic regions at least up to 50 °C. The surfactant−water and the surfactant−oil miscibility gaps determine the phase diagram pattern.[26] It was observed that the Myrj45 + *n*-PrOH combination at 1:2 weight ratio was soluble with oil and water at higher concentration. So, the 1ϕ (Winsor IV)[27] microemulsion region was more concentrated on the higher surfactant region of the phase diagram and started from the surfactant apex and extended toward the middle portion of the triangle. This region separates from the two phase Winsor I L/L (i.e., oil/microemulsion) system.[27] The area of this region does not change much with the variation of temperature (Table 1) probably because of an almost equal antagonistic effect of temperature on hydrophobicity/hydrophilicity of the ionic and nonionic surfactants. We had already studied the phase diagram of the system water/SDS + *n*-propanol/cyclohexane at 30, 40, and 50 °C[21] (see Figure 1a), and in this phase diagram the microemulsion zone was attached to a portion of the zero oil line of the phase diagram. Hence this 1ϕ area may be a direct continuation of the region of micelles existing in the water/surfactant/cosurfactant phase diagram, as reported earlier.[28] In contrast to this fact, this 1ϕ region does not coincide with the zero water line of the diagram, which is because of the insolubility of the ionic surfactant in the hydrophobic phase unless some amount of water is present. The portion above and below this microemulsion zone constitutes a solid−liquid (S/L) biphasic region and a liquid−liquid (L/L) biphasic region, respectively. Similar curves in Figures 1b,c were observed in different SDS:Myrj45 (1:3 and 3:1 by weight) ratios. The behavior of the mixture of two dissimilar surfactants is generally more complex.[29,30] In fact, this complexity develops because of their different phase behaviors. It is known for a long time that an increase of temperature makes nonionic surfactants more hydrophobic and ionic surfactants more hydrophilic.[31,32] Consequently, the phase behavior with respect to temperature will be expected to be opposite. When Myrj45 and SDS were mixed, the 1ϕ region was in the middle part of the phase diagram and the change in SDS:Myrj45 mixing ratios did not have much effect on the phase diagram except for 1:1 ratio. The solid/liquid biphasic region of the SDS system and large liquid/liquid biphasic region of Myrj45 was present for all three mixed

TABLE 1: Percentage Area of Various Phases of the Water/SDS + Myrj45/*n*-PrOH/Cyclohexane System

	303 K			313 K			323 K		
SDS:Myrj-45	1ϕ	S/L	L/L	1ϕ	S/L	L/L	1ϕ	S/L	L/L
1:0				29	22	49			
3:1	21	29	50	26	27	47	30	20	50
1:1	25	21	54	30	22	48	32	17	51
1:3	37	12	51	38	10	52	37	12	51
0:1	33		67	25		75	24		76

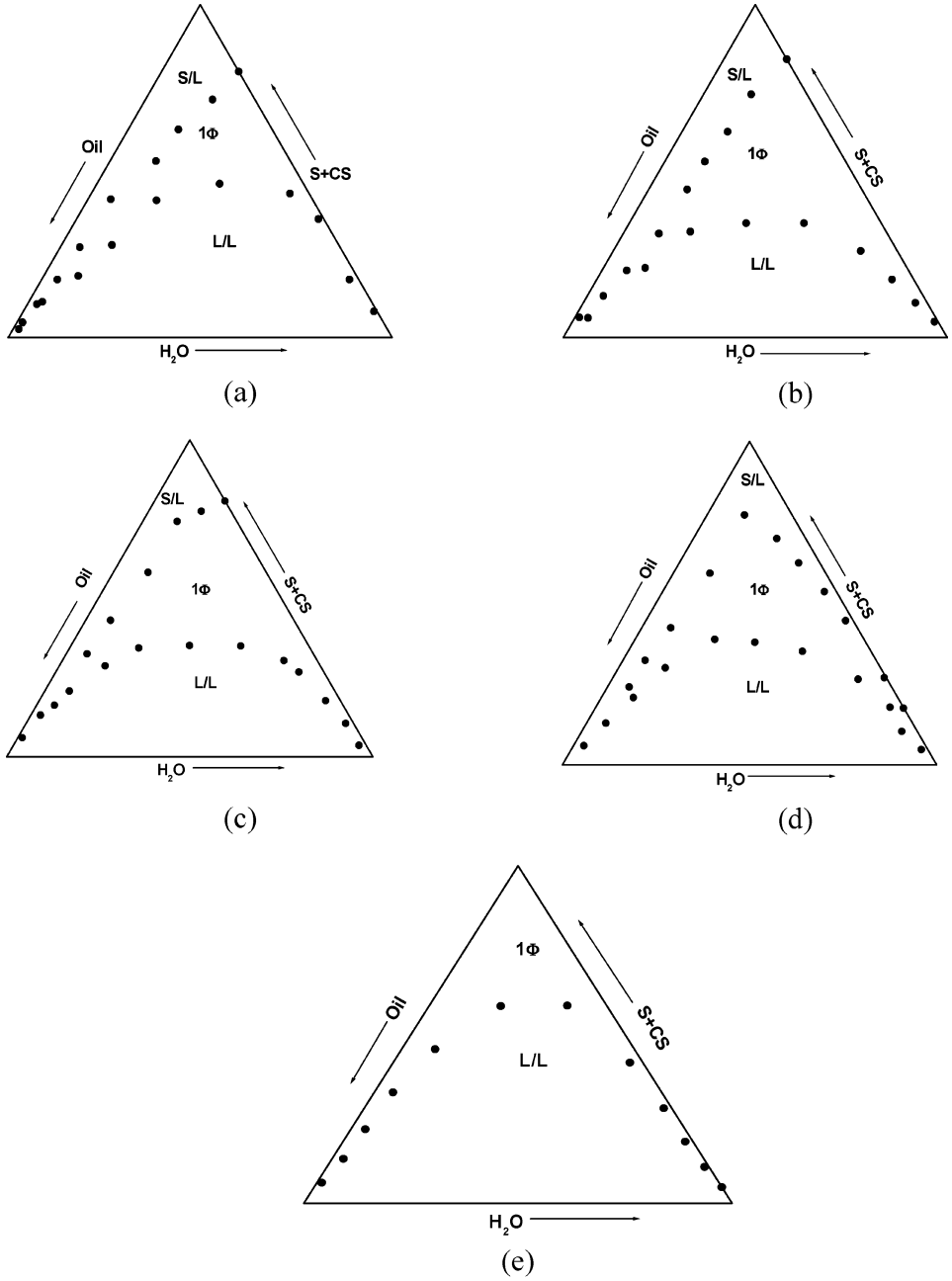

Figure 1. Phase diagrams of water/SDS + Myrj 45/*n*-PrOH/cyclohexane system at 40 °C with different SDS:Myrj 45 ratios (w/w): (a) 1:0; (b) 3:1; (c) 1:3; (d) 1:1; (e) 0:1. The S and CS are surfactants (pure or mixed) and cosurfactant, respectively, in this and subsequent figures.

surfactant ratios studied. The composition seems to have an effect on 1ϕ & 2ϕ (S/L) regions. 2ϕ L/L region seems to be independent of the surfactant composition. When two surfactants are mixed, depending on their chemical nature, they may form a new compound. If such compound is possible, then that will be in equilibrium with the surfactant molecules, which are in excess.[33] If the overall behavior of the newly formed surfactant as well as the other components is similar, then the system should show properties somewhat between the properties that were shown by pure components.[29,30] A close observation on the mixed surfactant system phase diagrams indicates that both surfactant molecules are not affecting each other's property significantly. It appears, therefore, that both surfactant molecules keep individual identity intact. This is possible only when there is practically no interaction between the two molecules. Hence we assume that there is no interaction between SDS and Myrj45 molecules here. This was also observed in the case of the SDS and Brij35 system studied by us earlier.[19] The alcohols generally assist the surfactant molecules to decrease the oil−water interfacial tension to very low values so that stabilization of microdroplets occurs and hence the formation of microemulsion (see Figure 2). By partitioning between aqueous and oil phases, alcohol molecules can modify the solvent properties of these two phases; i.e., it makes an aqueous phase comparatively more hydrophobic and an oil phase relatively more hydrophilic. That is why alcohols are useful in the μE formation. Figure 2 shows the IFT measured between the microemulsion (M) layer and equilibrated excess oil layer (O) or excess water layer (W) as a function of water−oil volume ratio for several systems. A longer chain length alcohol tends to promote a Winsor I → III → II transition. Alcohols also reduce the tendency to form liquid crystals. In other words, alcohols tend to reduce the chain−chain interaction energy of the amphiphiles, stabilizing the microemulsion and the solvency of the given amphiphile.[34] It is seen from Figure 2 that *n*-HexOH is a good cosurfactant for formation of a microemulsion (W III), as it reduces the

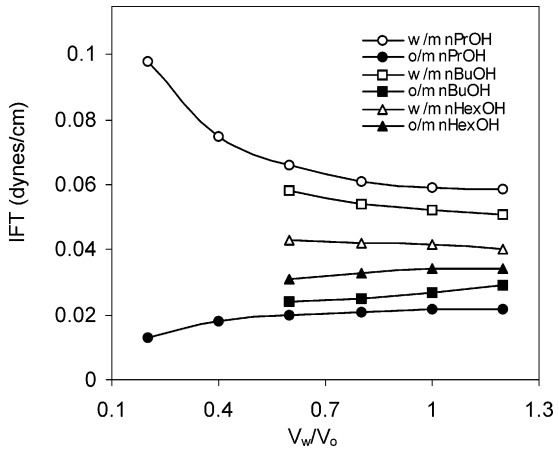

Figure 2. Variation of IFT as a function of the water/oil volume ratio for water/SDS + Myrj45/*n*-PrOH/cyclohexane at 29.4 °C.

difference in IFT between W/M and O/M considerably more as compared to *n*-PrOH and *n*-BuOH. It is obvious here that as the water volume increases, the IFT tends toward constancy. The IFT at the W/M interface is somewhat larger than that at the O/M interface. Further, Aveyard et al.[35] also studied the Winsor transitions and interfacial film compositions in systems containing sodium dodecylbenzenesulfonate and alkanols. They showed that inversion of microemulsion type (from o/w to w/o) could not be affected by addition of salt alone. The addition of alkanol as cosurfactant can promote the Winsor I → III → II transitions and reduce the oil−water IFT to ultralow values.

We also studied the effect of temperature change in the presence of 0.5, 0.8, and 1 M NaCl. Figure 3 shows solid/liquid phases at both lower and higher surfactant concentrations. The overall S/L area increases with an increase in temperature, indicating a decrease in surfactant solubility. The boundary line of the liquid/liquid phase at 30 °C significantly changes when 0.5 M NaCl is added to the system. The solid/liquid phase changes to a liquid crystalline phase when the temperature is lowered to below 283 K, which shows that the liquid crystalline phase melts at 283 K. The phase diagram of the cyclohexane/SDS + Myrj45 (1:1)/*n*-PrOH/0.5/0.8/1 M aqueous NaCl systems were determined at 30, 40, and 50 °C. In this case S/L areas show some change with change in NaCl concentration (Figure 4). The three phase (3ϕ) Winsor III[27] system (the system in which the microemulsion is in equilibrium with both oil and water) area increases slightly with an increase in temperature. At 30 °C there is no 3ϕ system in the presence of 0.5 M NaCl whereas at 40 and 50 °C such systems are present, with a little larger area at 50 °C. The increase in the three-phase (3ϕ) area in the phase diagram may also be due to microstructural changes with the rise of temperature. A microstructural transition in a microemulsion is based on the interfacial surfactant film. The values of the spontaneous curvature C_o indicate whether the surfactant film is bent toward oil or water.[36] However, when the value tends toward zero, a bicontinuous structure is observed.[37] Aveyard et al.[38] have proposed that the nature of C_o can be obtained from the geometrical tail (A_t) and head (A_h) areas of the surfactant. For ionic surfactants in water the C_o is positive because of the high repulsive forces between headgroups and an o/w microemulsion is generally ensured. Addition of NaCl is expected to decrease the repulsive force, and thereby C_o may be zero or even negative. That is, transition from o/w to bicontinuous to w/o microemulsion structure can be obtained. For nonionic surfactants, due to the hydration of the headgroups, the heads are far apart and C_o is positive. An increase in temperature decreases the hydration and hence C_o.[37] That is,

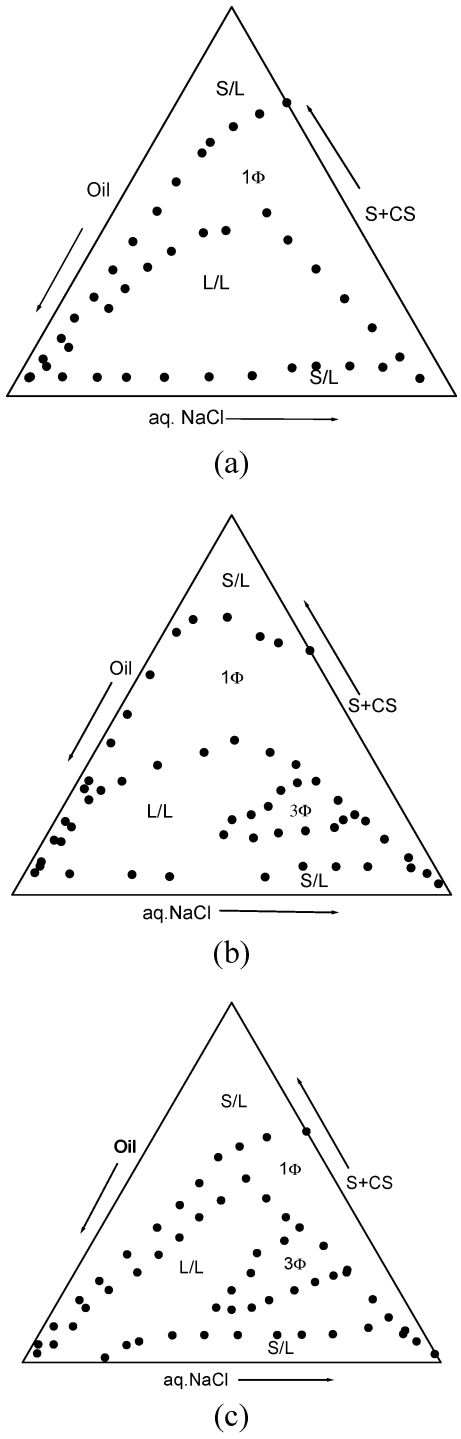

Figure 3. Phase diagrams of the aqueous NaCl (0.5 M)/SDS + Myrj 45 (1:1)/*n*-PrOH/cyclohexane system at different temperatures: (a) 30 °C; (b) 40 °C; (c) 50 °C.

an increase in temperature and addition of NaCl have similar effects on the microstructure of microemulsion. The phase diagram of SDS/cyclohexane with 0.5 M aqueous NaCl solution is similar to the phase diagram of the same system in the absence of NaCl.[22] However, an ∼20% increase in the area of the 1ϕ microemulsion is observed. The ionic surfactant, because of its high hydrophilicity, does not form a 3ϕ microemulsion. The presence of an electrolyte like NaCl decreases the hydrophilicity and hence the possibility of the formation of 3ϕ Winsor III system. The presence of electrolyte reduces the repulsive interaction between charged surfactant molecules and hence affects the phase diagram.[39] The volume fractions of various

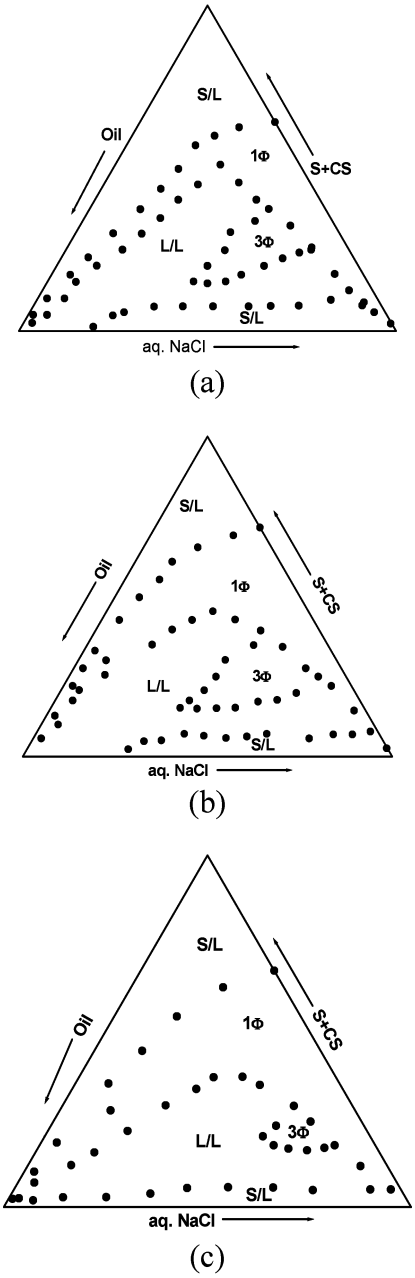

Figure 4. Phase diagrams of the aqueous NaCl/SDS + Myrj 45 (1:1)/*n*-PrOH/cyclohexane system at 50 °C temperature at different NaCl concentrations: (a) 0.5 M; (b) 0.8 M; (c) 1.0 M.

layers formed, for a composition (arbitrarily taken) S + CS (17.5%), oil (42.3%), and water (40.2%), show that the system is biphasic at all temperatures studied up to 0.5 M NaCl with μE at the bottom and excess oil at the top. At concentrations above 0.5 M, there appears 3ϕ, the lower one is aqueous, the upper one is oil, and the middle phase is bicontinuous μE. On a further increase in NaCl concentration, the μE phase increases at the expense of the upper oil phase. At a still higher concentration of NaCl (~1.2 M) the system reverts back to a biphasic one with the microemulsion at the top and water at the bottom at all temperatures (Winsor II). In Figure 5 detailed studies of Winsor transitions, carried out in different SDS:Myrj45 mixed systems are presented. Comparing the above results with the Sabatini et al.[39] equation

$$H = C|\ln m^*/m| \qquad (2)$$

where H is curvature, C is the proportionality constant, m^* is the optimum salinity, and m is electrolyte concentration, it was observed that Winsor transitions in the present case are as expected from eq 2 (i.e., Winsor I → III → II) as the NaCl concentration increases. According to them, when the electrolyte concentration (m) is less than the optimum salinity (m^*), then the quantity H is positive, which corresponds to a positive curvature and the μE is oil in water. When $m^* = m$, the logarithm is zero, which corresponds to a bicontinuous microemulsion, and when $m^* < m$, the logarithm is negative and corresponds to the formation of water in oil (Winsor II). However, we find that for our system the μE is spread over a concentration range from $m < m^*$ to $m > m^*$ before we get the o/w and w/o μE only. One could measure the volumes of oil, water, and microemulsion, i.e., V_o, V_w, and V_m, respectively, at each condition. The solubilization parameter V_o/V_m for oil and V_w/V_m for water can be plotted together against NaCl concentration (Figure 6). The concentration of NaCl at which these two curves intersect is termed the optimal salinity. We could obtain the optimum salinity only at 40 and 50 °C for SDS and Myrj 45 at various weight ratios (Figure 7). As revealed from the graph (Figure 7) the higher the SDS content, the higher is the optimum salinity. The optimal salinity is lower at low SDS mole fraction and becomes roughly constant at a higher mole fraction of SDS (X_{SDS}). At the optimal salinity, the volume of oil and the volume of water are the same in the microemulsion. However, the total microemulsion volume also changes with a change in X_{SDS} values. In our earlier papers[22,23] we have shown that the optimum salinity is a function of temperature, and both an increase[23] and a decrease[22] were observed depending on the cosurfactant used. The optimum salinity seems to be a function of the HLB of the system, which changes with temperature; hence the above observation.

Percolation Studies

A steep rise in conductance to an extent of ~6 orders of magnitude on a small change in water concentration above a threshold water volume fraction, characteristic of percolation phenomenon, can be observed in all plots (Figure 8a,b). The conductance remains very low initially and rapidly attains a high value, whose onset occurs at higher values of the water fraction, on increasing the chain length of the alcohols. Above the water percolation threshold the conductance rises sharply with the increase of water volume fraction, because of an efficient transfer of ions through the water phase. Also, the interaction between droplets plays a major role in producing the percolation effect. Depending on the droplet−droplet interaction, the percolation threshold value can vary. This value decreases when droplet−droplet interaction increases. As the chain length of alcohol increases, the droplet−droplet interaction decreases and hence the percolation threshold increases. There are at least two different mechanisms to explain the percolation phenomenon.[40] The first model, i.e., static percolation, is attributed to the transformation into a bicontinuous structure where the water channels are present whereas in the dynamic percolation model attractive water globule−globule interactions leading to cluster formation are suggested. A pictorial view has been suggested by Moulik et al.[41]

As the water concentration increases, the population of water globules increases and hence the possibility of the increase in conductance. The low conductance exhibited by w/o microemulsion is mainly due to a dynamic hoping mechanism[40] of ions through the globules whereas above the percolation threshold a sticky collision leading to the droplet fusion holds

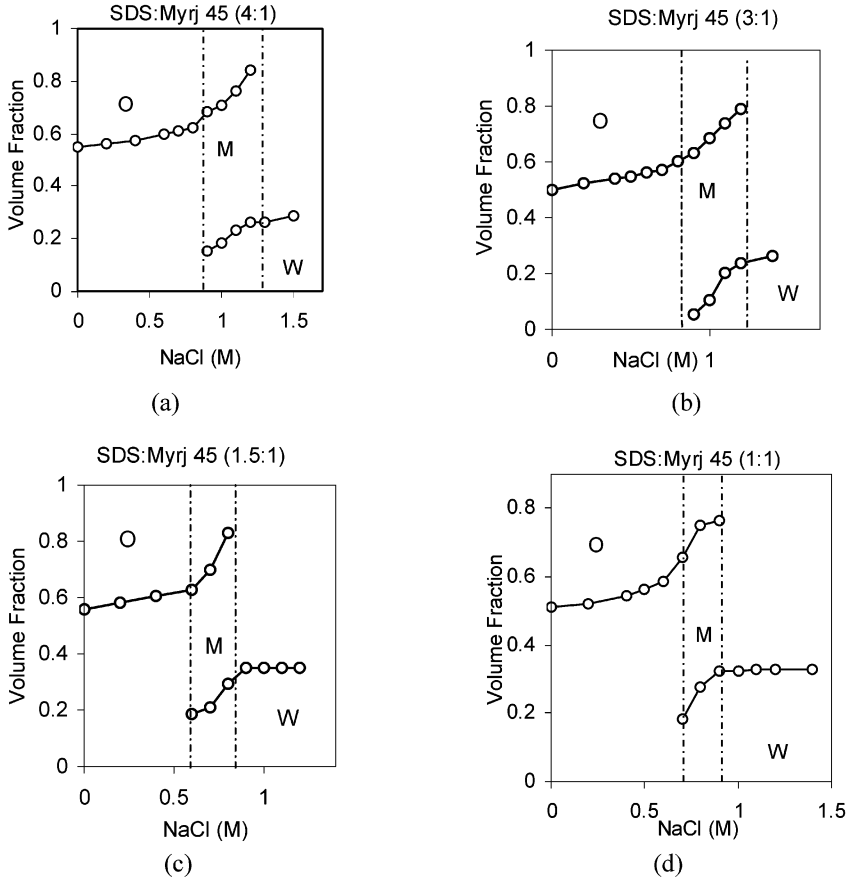

Figure 5. Plots of the volume fraction of different layers vs NaCl concentration for the composition S + CS (17.5%), oil (42.3%), and water (40.2%) in the mixed system at 50 °C temperature at different SDS:Myrj 45 ratios: (a) 4:1; (b) 3:1; (c) 1.5:1; (d) 1:1.

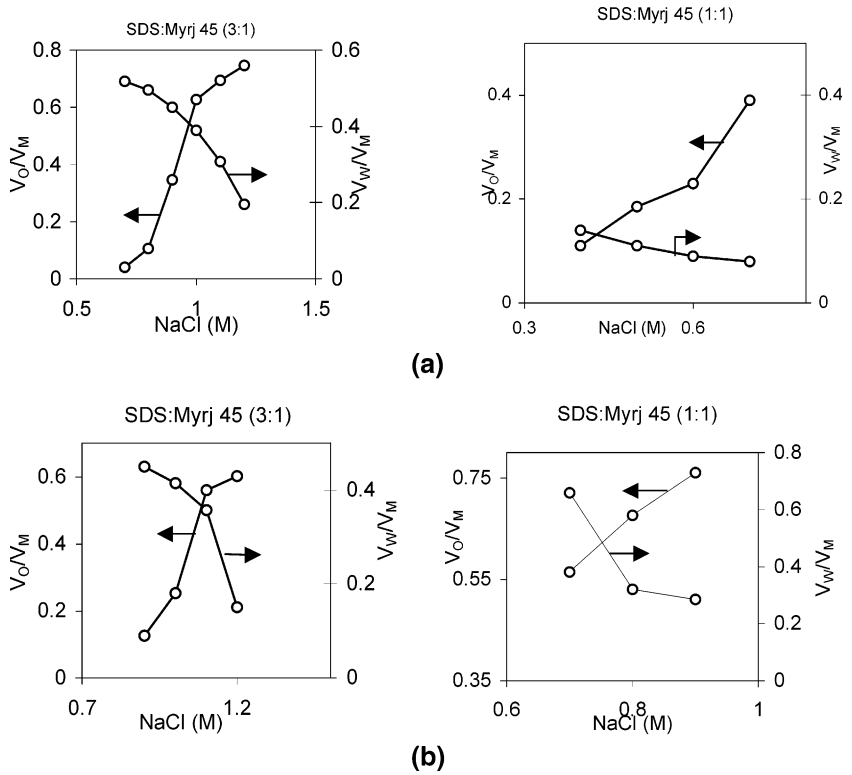

Figure 6. Plots showing the salinity scan for the system water/SDS + Myrj 45/*n*-PrOH/cyclohexane for 3:1 and 1:1 ratios at (a) 40 °C and (b) 50 °C. For composition see Figure 5.

the responsibility. It was also seen that sometimes a decrease in temperature or pressure for systems with the ionic[8,17] and nonionic surfactants[29] leads to a significant increase of the specific conductance. Because as temperature increases, there is increased kinetic energy of the water droplets in the oil continuum. Hence each droplet spends less time in the vicinity

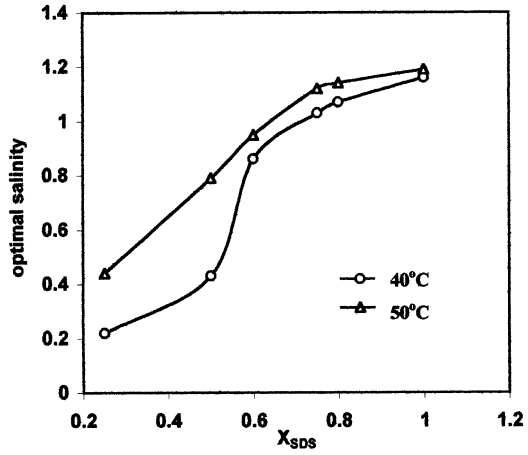

Figure 7. Plot of optimum salinity for the system water/SDS + Myrj 45/*n*-PrOH/cyclohexane vs mole fraction of SDS at different temperatures. For composition see Figure 5.

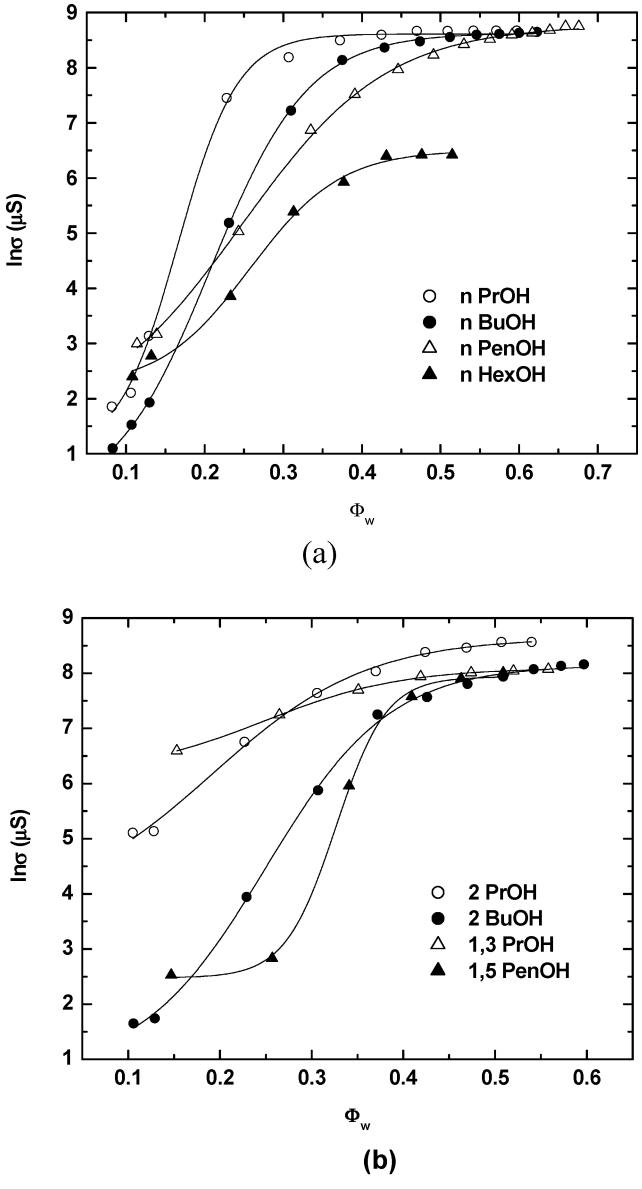

Figure 8. ln σ vs ϕ_w profile of water/SDS + Myrj 45 (1:1)/cyclohexane in the presence of different alcohols at 30 °C.

of another droplet at low w/o ratios while they collide. If this time span is much less than the time required for hoping, then there is a decrease in the probability of the conducting ions to hop along from globule to globule and hence low conductance. Thus a decrease in conductance with an increase in temperature supports the hoping mechanism rather than the sticky collision. In the present case the effect of temperature on the conductance of a w/o microemulsion at [H_2O]/[surf] mole ratio $w = 21.9$ is exemplified in Figure 9. The curves supports the absence of temperature-induced percolation, as also shown by some aliphatic hydrocarbon systems.[42] The effect of the temperature on the phase behavior of the systems studied here was found to be insignificant. Normally, both water- and temperature-induced percolations are witnessed in practice.[43] Here, we found systems that deviated from expectation probably because of too high an energy barrier for droplet cluster to occur.

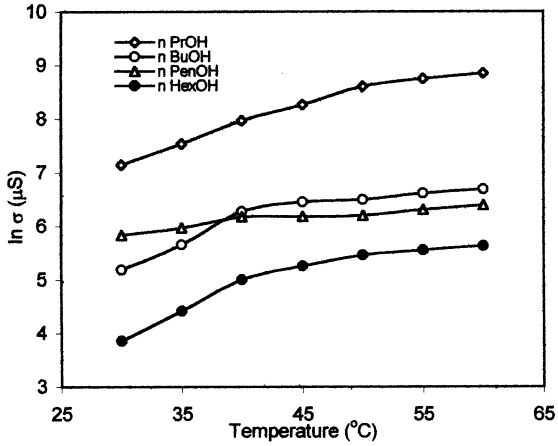

Figure 9. Plot of ln σ vs temperature of water/SDS + Myrj 45 (1:1)/cosurfactant/cyclohexane system at [H_2O]:[surf] = ~22 for different cosurfactants.

The threshold volume fraction (ϕ_w^p) of the dispersed phase required for the onset of percolation is usually determined from the differential plot (d ln σ/dϕ_w), which shows a peak in the plot[44] corresponding to ϕ_w (volume fraction of water). Very recently, the use of the sigmoidal Boltzmann equation (SBE) for the determination of the threshold volume (ϕ_w^p) was proposed by Hait et al.[44] The SBE equation is in the form

$$\log \sigma = \frac{\log \sigma_i - \log \sigma_f}{[1 + \exp(\phi_w - \phi_w^p)]/d\phi_w} + \log \sigma_f \qquad (3)$$

where σ and ϕ_w represent conductance and volume fraction, respectively, and the subscripts i, f, and p are for initial, final, and percolation stages, respectively. The threshold values at different temperatures in different alcohols are given in Table 2. From this table as well as Figure 8, it is observed that ϕ_w^p increases as the alkyl chain length of alcohol increases and ϕ_w^p decreases with increasing temperature.

The general increase in ϕ_w^p values with increasing alcohol chain length (Table 2) reveals the increased necessity for the water phase to form water channels through which the ion transport can occur. In other words, the droplets undergo less favorable sticky collisions at low water concentration in the presence of higher alcohols and merge to form the conduits that are the pathway for exchange of ions. This is expected, as the hydrophobic groups of alcohol will be at the boundary of the water droplet. This is also seen from the light scattering studies,[45−48] where it is seen that the interdroplet attractive interaction in the w/o microemulsion decreases when the alcohol chain length increases. Calculation of the interaction potential between the water droplets is based on the assumption that the attractive interactions between globules arise from the inter-

TABLE 2: Percolation Threshold, Scaling Law Parameters, and Activation Energies at the Percolation Threshold for Water-Induced Percolation of the Water/SDS + Myrj45 (1:1)/Cyclohexane Microemulsion System with Different Alcohols at Different Temperatures

alcohol	temp (K)	ϕ_w^p	ln k	n	E_p (kJ mol^{-1})
n-PrOH	303	0.166 ± 0.006	9.565 ± 0.110	0.742 ± 0.063	15.2
	313	0.113 ± 0.004	9.204 ± 0.046	0.621 ± 0.022	
	323	0.061 ± 0.011	9.904 ± 0.148	0.874 ± 0.069	
n-BuOH	303	0.208 ± 0.002	9.957 ± 0.141	1.214 ± 0.079	18.0
	313	0.156 ± 0.038	9.218 ± 0.108	1.201 ± 0.018	
	323	0.149 ± 0.041	9.207 ± 0.211	0.998 ± 0.038	
n-PenOH	303	0.247 ± 0.008	8.984 ± 0.031	0.642 ± 0.024	27.7
	313	0.190 ± 0.024	8.642 ± 0.004	1.639 ± 0.038	
	323	0.172 ± 0.008	8.639 ± 0.019	0.742 ± 0.149	
n-HexOH	303	0.257 ± 0.009	7.516 ± 0.189	0.731 ± 0.095	35.6
	313	0.212 ± 0.048	8.827 ± 0.309	1.221 ± 0.067	
	323	0.206 ± 0.016	8.014 ± 0.260	0.909 ± 0.125	
2-PrOH	303	0.192 ± 0.030	8.841 ± 0.280	0.847 ± 0.043	17.6
	313	0.162 ± 0.021	9.247 ± 0.110	0.908 ± 0.017	
	323	0.138 ± 0.036	9.810 ± 0.169	1.142 ± 0.032	
2-BuOH	303	0.250 ± 0.006	9.416 ± 0.243	0.963 ± 0.032	24.0
	313	0.176 ± 0.042	9.599 ± 0.311	1.342 ± 0.015	
	323	0.149 ± 0.039	9.989 ± 0.200	0.174 ± 0.051	
1,3-PrOH	303	0.249 ± 0.008	9.249 ± 0.110	0.802 ± 0.041	18.9
	313	0.205 ± 0.085	9.131 ± 0.169	1.142 ± 0.052	
	323	0.173 ± 0.025	8.998 ± 0.242	1.369 ± 0.032	
1,5-PenOH	303	0.326 ± 0.003	9.551 ± 0.184	0.845 ± 0.066	37.4
	313	0.267 ± 0.012	10.382 ± 0.469	1.244 ± 0.240	
	323	0.219 ± 0.047	10.605 ± 0.326	1.509 ± 0.157	

penetration of the droplet water cores close to each other. Also, according to Hou and Shah,[9] the interdroplet attractive interaction increases as the number of carbon atoms in alcohol (n_a) and/or the number of carbon atoms in the surfactant (n_s) (i.e., total number of carbon atoms in the system) decreases. As the shorter *n*-propanol molecules are replaced by longer *n*-hexanol molecules, the difference, i.e., $n_s - n_a$, decreases. Moreover, when the interfaces are packed with an increased number of longer alcohol chains, the surfactant tails get uncoiled and straighten up. These two effects make the interdroplet interaction low, and the system requires more water to form water channels. That is why increased ϕ_w^p is observed as we increase the alcohol chain length. It is evident from the results that, as we change the position of the hydroxyl group in the PrOH series, the percolation threshold increases, meaning more water is required to form water channels. The difference in the observed ϕ_w^p different alcohols could be due to changes in attractive interactions between the droplets. These interactions are also affected due to the different geometrical arrangement at the w/o interface for different alcohols.

The scaling laws[10]

$$\sigma \propto (\phi_w - \phi_w^p)^n \tag{4}$$

$$\ln \sigma = \ln k + n \ln(\phi_w - \phi_w^p) \tag{5}$$

where σ is the specific conductance of the microemulsion system, ϕ_w is the volume fraction of water in the system, ϕ_w^p is its volume fraction at the percolation threshold, k is the proportionality constant, and n is a constant in eq 4, have been used. k and n values are obtained from the ln σ vs ln($\phi_w - \phi_w^p$) plot and are given in Table 2, along with errors in the slope and intercept. The values of ln k and n fall in the range 8.01−10.64 and 0.62−1.64, respectively. The experimental value of n thus is lower than the predicted value of 1.9,[13] which is also seen in the literature.[43,49,50] This indicates that the percolation mechanism may not be as discussed and further work is required to explain this difference between the theory and experimental results. Moreover, it can be noted that there is no regular variation of ln k and n with temperature except in a couple of cases. This indicates that the percolation mechanism is a reasonably complicated one and is not as straightforward as is accepted at the moment. The possibility that both the suggested mechanisms are simultaneously present may be considered besides any other alternative mechanism. However, we have no alternative suggestion at the moment.

The activation energy (E_p) for conductance percolation has been computed using an Arrhenius type expression

$$\sigma = A e^{-E_p/RT} \tag{6}$$

where A is a constant, σ is the conductance at the percolation threshold (i.e., conductance corresponding to ϕ_w^p), and R and T have their usual significance. By using eq 3, the ln σ at ϕ_w^p was calculated at various temperatures for a particular cosurfactant and this ln σ was plotted against T^{-1}. Reasonably good straight lines were obtained and the slopes ($-E_p/R$) were calculated and hence E_p (Table 2). It is observed that as the chain length of CS increases, the E_p increases. A plot of E_p vs carbon number of CS shows a reasonably good straight line (Figure 10), indicating that percolation energy barrier increases by ∼6.6 kJ mol^{-1} per CH_2 group.

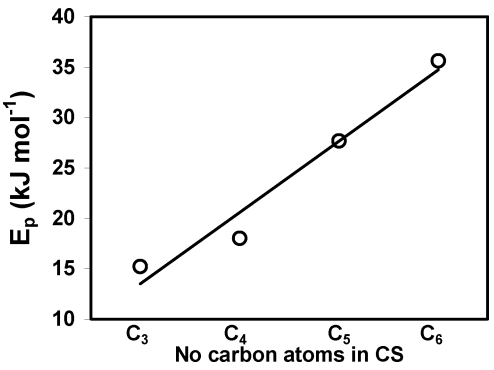

Figure 10. Plot of E_p against no. of carbon atoms of cosurfactants.

Conclusions

In the water/SDS + Myrj45 /*n*-PrOH/cyclohexane system, it was observed that when Myrj45 and SDS were mixed, the 1ϕ region was in the middle part and a change in SDS:Myrj45 mixing ratios did not have much effect on the phase diagram except for 1:1 SDS:Myrj45 ratio. Among alcohols *n*-HexOH was a good cosurfactant for formation of microemulsions, as it reduces the difference in IFT between O/M & W/M considerably as compared to lower homologs. NaCl introduced a three-phase zone in above microemulsion system. At higher temperatures the optimum salinity was higher. Water-induced percolation of water/SDS + Myrj45(1:1)/ *n*-PrOH/cyclohexane microemulsion system in the presence of different alcohols was investigated, and a higher ϕ_w^p was obtained for higher alcohols. This was associated with higher E_p values. The absence of temperature-induced percolation in the above system was witnessed.

Acknowledgment. Financial assistance from CSIR (ref no. 1(1706)/01/EMR-II) is gratefully acknowledged.

References and Notes

(1) Ruckenstein, E.; Chi, C. J. *J. Chem. Soc., Faraday Trans.* **1975**, *71*, 1960.
(2) DeGennes, P. G; Taupin, C. *J. Phys. Chem.* **1982**, *86*, 2294.
(3) Munoz, E.; Gomez-Herrera, C.; del Mar Graciani, M.; Moya, M. L.; Sanchez, F. *J. Chem. Soc., Faraday Trans.* **1991**, *87*, 129.
(4) Peyrelasse, J.; Mcclean, V. E. R.; Boned, C.; Sheppard, R. J.; Clausse, M. *J. Phys. D: Appl. Phys.* **1978**, *L117*, 11.
(5) Clausse, M.; Sheppard, R. J.; Boned, C.; Essex, C. G. *Colloid Interface Sci*. **1976**, *2*, 233.
(6) Hilfiker, R.; Eicke, H. F.; Geiger, S.; Furler, G. J. *J. Colloid Interface Sci* **1985**, *105*, 378.
(7) Jada, A.; Lang, J.; Zana, R. *J. Phys. Chem*. **1989**, *93*, 10.
(8) Ollson, U.; Wennerstrom, H. *Adv. Colloid Interface Sci*. **1994**, *49*, 113.
(9) Hou, M. S.; Shah, D. O. *Langmuir* **1987**, *3*, 1086.
(10) Lagourette, B.; Peyrelasse, J.; Boned, C.; Clausse, M. *Nature* **1979**, *281*, 60.
(11) Lagues, M.; Ober, R.; Taupin, C. *J. Phys. Lett*. **1978**, *39(L*), 489.
(12) Kirkpatrick, S. *Phys. Rev. Lett*. **1971**, *27*, 1722.
(13) Feldman, Y.; Kozlovich, N.; Nir, I.; Garti, N. *Phys. Rev. E* **1995**, *51*, 478.
(14) Ray, S.; Paul, S.; Moulik, S. P. *J. Colloid Interface Sci*. **1996**, *183*, 6.
(15) Dutkienicz, E.; Robinson, B. H. *J. Electroanal. Chem*. **1988**, 490.
(16) Lindaman, B.; Shinoda, K.; Ollson, U.; Anderson, D.; Karlstrom, G.; Wennerstrom, H. *Colloids Surf.* **1989**, *38*, 205.
(17) Ajith, S.; John, A. C.; Rakshit, A. K. *Pure Appl. Chem*. **1994**, *66*, 509.
(18) Ajith, S.; Rakshit, A. K. *J. Surf. Sci. Technol* **1992**, *8*, 365.
(19) Ajith, S.; Rakshit, A. K. *J. Phys. Chem.* **1995**, *99*, 14778.
(20) Ajith, S.; Rakshit, A. K. *Langmuir* **1995**, *11*, 1122.
(21) John, A. C.; Rakshit, A. K. *J. Colloid Interface Sci.* **1993**, *156*, 202.
(22) John, A. C.; Rakshit, A. K. *Langmuir* **1994**, *10*, 2084.
(23) John, A. C.; Rakshit, A. K. *Colloids Surf. A* **1995**, *95*, 201.
(24) Kahlweit, M.; Strey, R.; Haase, D.; Firman, P. *Langmuir* **1988**, *4*, 785.
(25) Findenegg, G. H.; Hirtz, H.; Rarch, R.; Sowa, F. *J. Phys. Chem*. **1989**, *93*, 4580.
(26) Kahlweit, M.; Lessner, E.; Strey, R. *J. Phys. Chem*. **1983**, *87*, 5032.
(27) Winsor, P. A. *Chem. Rev.* **1968**, *68*, 1.
(28) Boned, C.; Clausse, M.; Lagourette, B.; Peyrelasse, J.; Mcclean, V. E. R.; Sheppard, R. J. *J. Phys. Chem*. **1980**, *84*, 1520.
(29) Kunieda, H.; Hanno, K.; Vamaguchi , S.; Shinoda, K. *J. Colloid Interface Sci*. **1985**, *107*, 129.
(30) Graciaa, A.; Lachaise, J.; Bourrel, M.; Obsorne-Lee, I.; Schechter, R. S.; Wade, W. H. *J. Colloid Interface Sci.* 1**983**, *94*, 179.
(31) Schubert, K. V.; Busse, G.; Strey, R.; Kahlweit, M. *J. Phys. Chem*. **1993**, *97*, 248.
(32) Shinoda, K.; Kuneida, H.; Arai, T.; Saijo, H. *J. Phys. Chem*. **1984**, *88*, 5126.
(33) Anton, R. E.; Gomez, D.; Graciaa, A.; Lachaise, J.; Salager, J. L. *J. Dispersion Sci. Technol*. **1993**, *14*, 401.
(34) Lam,.C.; Falk, N. A.; Schechter, R. S. *J. Colloid Interface Sci.* **1987**, *120*, 30.
(35) Ahsan, T.; Aveyard, R.; Binks, B. P. *Colloids Surf*. **1991**, *52*, 339.
(36) Langevin, D. *Adv. Colloid Interface Sci.* **1991**, *34*, 583
(37) Safran, S. A. In *Micellar Solutions and Microemulsions: Structure, Dynamicc and Statistical Thermodynamics*; Chen, S. H., Rajagopalan, Rr., Eds.; Springer-Verlag: NewYork, 1990; p 165.
(38) Aveyard, R.; Binks, B. P.; Fletcher, P. D. I. In *The Structure, Dynamics and Equilibrium Properties of Colloidal Systems*; Bloor, D. H., Wyn-Jones, E., Eds.; Kluwer Academic Publishers: Norwell, MA, 1990; p 557.
(39) Acosta, E.; Szekeres, E.; Sabatini, D. A.; Harwell, J. H. *Langmuir* **2003**, *19*, 186.
(40) Ponton, A.; Bose, T. K.; Delbos, G. *J. Chem. Phys*. **1991**, *94*, 6879.
(41) Ray, S.; Paul, S.; Moulik, S. P. *J. Colloid Interface Sci.* **1996**, *83*, 6.
(42) Mukhopadhyay, L.; Bhattacharya, P. K.; Moulik, S. P *Colloids Surf*. **1990**, *50*, 295.
(43) Ray, S.; Moulik, S. P. *J. Phys. Chem.* **1990**, *94*, 421.
(44) Hait, S. K.; Moulik, S. P.; Rodgers, M. P.; Burke, S. E.; Palepu, R. *J. Phys. Chem.* **2001**, *105*, 7145.
(45) Cazabat, A. H.; Chatenay, D.; Langevin, D.; Pouchelon, A. *J. Phys. Lett.* **1980**, *41*, 441.
(46) Hou, M. J.; Kim, M.; Shah, D. O. *J. Colloid Interface Sci.* **1988**, *123*, 398.
(47) Brunetti, S.; Roux, D.; Bellocq, A. H.; Fourche, G.; Bothorel, P. *J. Phys. Chem.* **1983**, *87*, 1028.
(48) Lemaire, B.; Bothorel, P.; Roux, D. *J. Phys. Chem.* **1983**, *87*, 1023.
(49) Ray, S.; Bisal, S. R.; Moulik, S. P. *J. Chem. Soc., Faraday Trans* **1993**, *89*, 3277.
(50) Mitescu, C. D.; Musolf, M. J. *J. Phys. Lett. L* **1983**, 679.